Table 5. *Electrostatic balance*

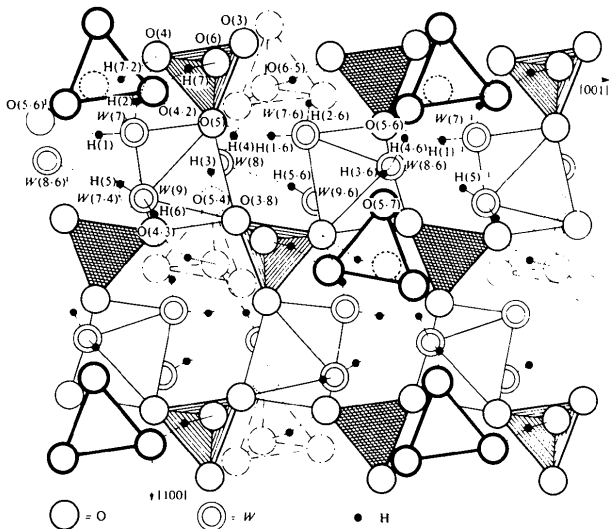|	O(3)	O(4)	O(5)	O(6)	W(7)	W(8)	W(9)	Σs_i
P	1·40	1·26	1·27	1·07				5·00
Mg	0·40	0·35	0·36		0·32	0·33	0·32	2·08
H(1)			0·18		0·82			1·00
H(2)		0·14			0·86			1·00
H(3)			0·15			0·85		1·00
H(4)				0·22		0·78		1·00
H(5)						0·07	0·93	1·00
H(6)					0·04	0·03	0·93	1·00
H(7)		0·28		0·72				1·00
Σs_i	1·80	2·03	1·96	2·01	2·04	2·06	2·18	

Fig. 3. Hydrogen-bond network in newberyite; projection along [0Ī0].

The electrostatic balance for O atoms corresponds to the expected values according to the Pauling rules except for O(3) and $W(9)$, which are underbonded ($s_i = 1·80$) and overbonded ($s_i = 2·18$) respectively. The P–O(3) distance (1·500 Å) is one of the shortest found in orthophosphate groups. The underbonding of the O atom, which is usually observed in these cases, suggests some limited validity of Brown & Shannon's formula for short or very short bond distances. O(3) is the only O atom which is not an acceptor of a H bond; it has the strongest bond with P and Mg.

The difference in bond distances between Mg–O (average: 2·048 Å) and Mg–W (average: 2·107 Å) (Table 3) is due to the underbonding of O atoms [especially O(3)], which demands an approach of these atoms to the P and Mg atoms with respect to the water molecules, which exchange a small bond valence through their generally long H bonds.

References

BAUR, W. H. (1974). *Acta Cryst.* B30, 1195–1215.
BROWN, I. D. (1976). *Acta Cryst.* A32, 24–31.
BROWN, I. D. & SHANNON, R. D. (1973). *Acta Cryst.* A29, 266–282.
CATTI, M. & FERRARIS, G. (1973). *Acta Cryst.* B29, 90–96.
COHEN, L. H. & RIBBE, P. H. (1966). *Am. Mineral.* 51, 1755–1765.
CROMER, D. T. & WABER, J. T. (1974). *International Tables for X-ray Crystallography*, Vol. IV. Birmingham: Kynoch Press.
DE SCHULTEN, M. A. (1903). *Bull. Soc. Fr. Minéral. Cristallogr.* 26, 24–29.
FERRARIS, G. & FRANCHINI-ANGELA, M. (1972). *Acta Cryst.* B28, 3572–3583.
MOORE, F. H. (1963). *Acta Cryst.* 16, 1169–1175.
STOUT, G. H. & JENSEN, L. H. (1968). *X-ray Structure Determination*. New York: Macmillan.
SÜCKER, I. (1963). *Naturwissenschaften*, 50, 499–500.
SUTOR, D. J. (1967). *Acta Cryst.* 23, 418–422.
SUTOR, D. J. (1968). *Nature (London)*, 218, 295.
SUTOR, D. J., WOOLEY, S. E. & JACKSON, O. F. (1970). *Res. Vet. Sci.* 11, 298–299.
WHITAKER, A. (1968). *Mineral. Mag.* 36, 820–824.

The Structure of Potassium Tantalum Fluoride Oxide K₁₂Ta₁₅·₅F₁₈·₅O₃₅·₅

BY A. BOUKHARI, J. P. CHAMINADE, M. POUCHARD AND M. VLASSE

Laboratoire de Chimie du Solide du CNRS, Université de Bordeaux I, 351 cours de la Libération, 33405 Talence CEDEX, France

Abstract

The structure of $K_{12}Ta_{15.5}F_{18.5}O_{35.5}$ has been determined and refined in space group $P6$ to an R of 0·063.

It can be described as a three-dimensional framework formed by the interpenetration of two distinct sublattices with the formulations $[Ta_5 X_{17}]_{3n}$ and $[Ta_{0.5} X_3]_n$ ($X = $ O, F). The $[Ta_5 X_{17}]_{3n}$ skeleton is formed entirely of

TaX_6 octahedra demarking infinite complex tunnels in which are inserted the K^+ ions. The $[Ta_{0.5}X_3]_n$ sublattice is an infinite chain of trigonal prisms. [Crystal data: $a = 19.32$ (1), $c = 3.878$ (8) Å; $Z = 1$, $d_{exp} = 5.59$ (5), $d_c = 5.55$ Mg m^{-3}.]

Structures related to the tungsten-bronze types (HTB and TTB)* are made of a triangular motif (B_3X_{15}) of three BX_6 octahedra sharing common corners. These elementary blocks can be joined together by common corners, in parallel planes, giving rise to complex structures with infinite tunnels normal to these sheets of octahedra. The tunnels are generally hosts for monovalent or divalent cations.

Materials having such tunnel structures may be particularly suitable for fast-ion transport in so far as they offer to the inserted ion various degrees of freedom (Pouchard & Hagenmuller, 1978).

In a general study of the quarternary system A^I-B^V- O–F (A = Li, Na, K, Ag; B = Nb, Ta), several new phases have been prepared and characterized (Vlasse, Chaminade & Pouchard, 1973, 1976; Chaminade, Vlasse, Pouchard & Hagenmuller, 1974; Vlasse, Chaminade, Massies & Pouchard, 1975; Vlasse, Chaminade, Saux & Pouchard, 1977). In the system K–Ta–O–F three new phases have been prepared with hexagonal symmetry and the same c_0 parameter ($\simeq 3.90$ Å) (Vlasse, Boukhari, Chaminade & Pouchard, 1979; Boukhari, Chaminade, Vlasse & Pouchard, 1979). The octahedral frameworks of the phases $K_6Ta_{6.5}F_{9.5}O_{14.5}$ and $K_2Ta_4F_4O_9$ contain infinite tunnels, in which are inserted the K^+ ions. The present work deals with the structural study of the third phase $K_{12}Ta_{15.5}F_{18.5}O_{35.5}$.

Experimental

Single crystals were obtained by reacting appropriate quantities of K_2TaF_7, $KTaO_3$ and Ta_2O_5 in a sealed gold tube heated between 973 and 1173 K. The melt was then cooled slowly, giving rise to small needle-like crystals.

Hexagonal symmetry and possible space groups $P6$, $P\bar{6}$ or $P6/m$ were indicated by Weissenberg and precession photographs. The cell parameters refined from Guinier data are: $a = 19.32$ (1), $c = 3.878$ (8) Å (Cu $K\alpha_1$, $\lambda = 1.5405$ Å); $d_{exp} = 5.59$ (5) and, for $Z = 1$, $d_c = 5.55$ Mg m^{-3}.

A single crystal in the form of a small cylinder (0.23 × 0.02 mm) was used for data collection. The intensities were measured on a three-circle automatic diffractometer (Enraf–Nonius CAD-3) with Mo $K\alpha_1$

* HTB: hexagonal tungsten bronze; TTB: tetragonal tungsten bronze.

graphite-monochromated radiation ($\lambda = 0.70929$ Å) and a multiple $\theta/2\theta$ scanning technique up to $\theta_{max} = 35°$. Three standard reflexions were measured for every batch of 50 reflexions with no significant fluctuation in their intensities. 810 symmetry-independent reflexions were measured [$I \geq 3\sigma(I)$] and were corrected for Lorentz and polarization factors, but not for absorption [μ(Mo $K\alpha$) = 39.53 mm^{-1}].

Structure determination

The coordinates of five atoms [Ta(1)–Ta(5)] were obtained from a Patterson synthesis. Subsequent Fourier and difference syntheses revealed the positions of the K, X (X = O, F) and Ta(6) atoms. Refinement by isotropic, then anisotropic full-matrix least squares (Busing, Martin & Levy, 1962) led to a final $R = \sum ||F_o| - |F_c||/\sum |F_o| = 0.063$.* The space group $P\bar{6}$ was used throughout since it is the only one permitting the present atomic arrangement inside the tunnels. A final difference synthesis showed no significant residual electron density.

Scattering factors were those of McMaster, Kerr del Grande, Mallet & Hubbel (1969), and the anomalous-dispersion corrections those of Dauben & Templeton (1962).

The final positional and thermal parameters are given in Table 1. Table 2 gives the interatomic distances.

Description and discussion of the structure

A projection of the structure perpendicular to (001) is given in Fig. 1.

The structure can be described as the interpenetration of two sublattices with the formulas $[Ta_5 X_{17}]_{3n}$

* A list of structure factors has been deposited with the British Library Lending Division as Supplementary Publication No. SUP 34669 (6 pp.). Copies may be obtained through The Executive Secretary, International Union of Crystallography, 5 Abbey Square, Chester CH1 2HU, England.
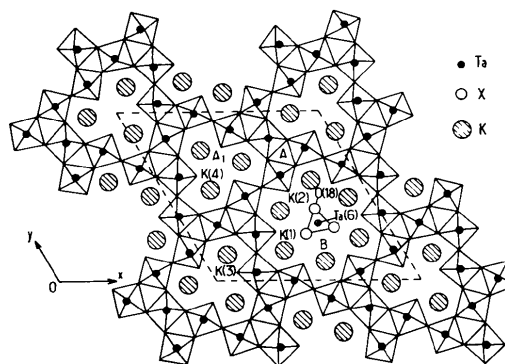

Fig. 1. Projection of the structure on the (001) plane showing the octahedral framework.

Table 1. *Atomic coordinates and thermal parameters of* $K_{12}Ta_{15.5}F_{18.5}O_{35.5}$, *with e.s.d.'s in parentheses*

	Site	x	y	z	$\beta_{11}(\times 10^5)^*$	$\beta_{22}(\times 10^5)$	$\beta_{33}(\times 10^5)$	$\beta_{12}(\times 10^5)$
Ta(1)	3(k)	0·3227 (3)	0·2764 (4)	$\frac{1}{2}$	0 (14)	11 (14)	1221 (372)	10 (12)
Ta(2)	3(k)	0·1641 (6)	0·3282 (6)	$\frac{1}{2}$	48 (15)	20 (18)	2298 (275)	10 (14)
Ta(3)	3(k)	0·0062 (6)	0·3859 (6)	$\frac{1}{2}$	85 (21)	93 (21)	5118 (710)	44 (17)
Ta(4)	3(k)	0·3824 (6)	0·4953 (5)	$\frac{1}{2}$	132 (24)	83 (22)	3796 (704)	73 (19)
Ta(5)	3(k)	0·2265	0·0500 (5)	$\frac{1}{2}$	36 (16)	35 (18)	2764 (523)	24 (16)
Ta(6)†	2(i)‡	0·6667	0·3333	0·373 (5)	96 (26)	96 (26)	4349 (1052)	48 (13)

	Site	x	y	z	B (Å^2)		Site	x	y	z	B (Å^2)
K(1)	3(j)	0·416 (2)	0·176 (2)	0	1·90 (1)	X(8)	3(k)	0·383 (8)	0·393 (7)	$\frac{1}{2}$	2·69 (2)
K(2)	3(j)	0·516 (2)	0·408 (2)	0	1·92 (1)	X(9)	3(k)	0·108 (9)	0·389 (9)	$\frac{1}{2}$	2·85 (3)
K(3)	3(j)	0·123 (1)	0·150 (2)	0	1·09 (1)	X(10)	3(k)	0·263 (10)	0·439 (8)	$\frac{1}{2}$	3·73 (5)
K(4)	3(j)	0·234 (2)	0·533 (2)	0	1·89 (1)	X(11)	3(k)	0·056 (10)	0·505 (9)	$\frac{1}{2}$	3·49 (5)
X(1)	3(k)	0·119 (10)	0·049 (9)	$\frac{1}{2}$	2·54 (2)	X(12)	3(k)	0·214 (10)	0·623 (9)	$\frac{1}{2}$	2·54 (2)
X(2)	3(k)	0·274 (10)	0·169 (9)	$\frac{1}{2}$	3·49 (5)	X(13)	3(j)	0·199 (5)	0·045 (6)	0	2·76 (2)
X(3)	3(k)	0·324 (8)	0·054 (8)	$\frac{1}{2}$	2·69 (3)	X(14)	3(j)	0·394 (6)	0·012 (6)	0	3·09 (5)
X(4)	3(k)	0·479 (9)	0·100 (9)	$\frac{1}{2}$	2·69 (3)	X(15)	3(j)	0·163 (6)	0·313 (5)	0	1·81 (2)
X(5)	3(k)	0·066 (9)	0·233 (8)	$\frac{1}{2}$	3·19 (5)	X(16)	3(j)	0·323 (5)	0·284 (5)	0	1·37 (2)
X(6)	3(k)	0·227 (10)	0·274 (10)	$\frac{1}{2}$	2·85 (3)	X(17)	3(j)	0·392 (6)	0·496 (6)	0	2·04 (2)
X(7)	3(k)	0·431 (9)	0·284 (10)	$\frac{1}{2}$	2·69 (2)	X(18)	3(j)	0·575 (6)	0·272 (7)	0	4·27 (8)

* The temperature factor expression is $\exp|-10^{-5}(h^2\beta_{11} + k^2\beta_{22} + l^2\beta_{33} + 2hk\beta_{12} + 2hl\beta_{13} + 2kl\beta_{23})|$.
† Occupancy factor for Ta(6): 0·25.
‡ For site 2(i): $\beta_{11} = \beta_{22} = 2\beta_{12}$.

and $[Ta_{0.5}X_3]_n$ (with $[Ta_5X_{17}]_{3n}$ + $[Ta_{0.5}X_3]_n$ = $[Ta_{15.5}X_{54}]_n$). Similar interpenetrating sublattices were found in $K_6Ta_{6.5}F_{9.5}O_{14.5}$ (Vlasse, Boukhari, Chaminade & Pouchard, 1979). The three-dimensional skeleton $[Ta_5X_{17}]_{3n}$ is formed entirely of TaX_6 octahedra, while the sublattice $[Ta_{0.5}X_3]_n$ is an infinite chain of trigonal prisms.

The K$^+$ ions are found in the tunnels of the $[Ta_5X_{17}]_{3n}$ skeleton and assure the cohesion between both sublattices.

The sublattice $[Ta_5X_{17}]_{3n}$

This sublattice is the basic framework of the structure. The Ta atoms adopt a slightly distorted octahedral coordination. A triangular $[Ta_3X_{15}]$ block made of three TaX_6 octahedra merges together with a similar one by sharing a common octahedron to give the $[Ta_5X_{24}]$ group (Fig. 2). Three such groups are linked together, each sharing two common corners. They give rise to a complex ring $[Ta_5X_{23}]_3$. These rings are put together to form an infinte $[Ta_5X_{22}]_{3n}$ sheet parallel to (001). These slabs are then stacked one upon the other along z by sharing their axial vertices. This infinite stacking results in the three-dimensional skeleton $[Ta_5X_{17}]_{3n}$ in which are found three types of tunnels directed along [001] (Fig. 1).

The tunnels with a triangular cross section (A in Fig. 1) are too small to allow the insertion of large atoms such as K, and are found to be empty. However, they could contain atoms such as Li or Ta as was shown in other phases by Perron-Simon, von der Mühll, Ravez & Hagenmuller (1977) and Awadalla & Gatehouse (1978).

The tunnels A_1 (Fig. 1) having a complex cross section contain three K$^+$ ions and are identical to those found in $K_2Ta_4F_4O_9$ (Boukhari, Chaminade, Vlasse & Pouchard, 1979). The second type of complex tunnel (B in Fig. 1) contains the infinite chain $[Ta_{0.5}X_3]_n$ and six additional K$^+$ ions. This type of tunnel with the associated infinite chain is similar to those of $K_6Ta_{6.5}F_{9.5}O_{14.5}$ (Vlasse, Boukhari, Chaminade & Pouchard, 1979).

The Ta–X distances in the $[Ta_5X_{17}]_{3n}$ framework range from 1·800 to 2·067 Å, with average distances of 1·915, 1·957, 1·967, 1·944 and 1·976 Å respectively for Ta(1), Ta(2), Ta(3), Ta(4) and Ta(5). By comparison, average distances in $K_2Ta_4F_4O_9$ are 1·965 and 1·957 Å, whereas for $K_6Ta_{6.5}F_{9.5}O_{14.5}$ they are 1·947 and 1·944 Å.

The K$^+$ ions have either six- or eightfold coordination. K(1) and K(3) are situated in a bicapped trigonal prism with average K$-X$ distances of 2·874 and 2·918 Å respectively. On the other hand, the coordination polyhedron of K(2) and K(4) is a simple
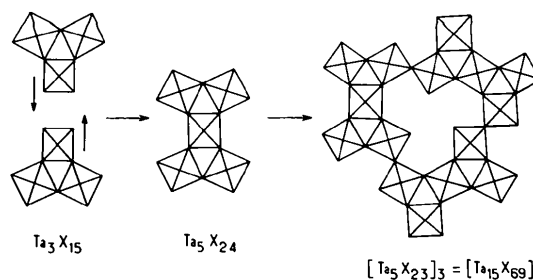

Ta_3X_{15} Ta_5X_{24}

$[Ta_5X_{23}]_3 = [Ta_{15}X_{69}]$

Fig. 2. Formation of the ring $[M_5X_{23}]_3$ from the basic unit $[M_3X_{15}]$.

Table 2. *Interatomic distances* (Å) *with e.s.d.'s in parentheses*

Ta(1)—X(2)	1·800 (12)	Ta(4)—X(8)	1·982 (10)
—X(6)	1·826 (13)	—X(10)	1·999 (12)
—X(7)	2·023 (12)	—X(11ⁱ)	1·884 (12)
—X(8)	1·951 (9)	—X(12)	1·903 (12)
—X(16)	1·944 (6) [2]*	—X(17)	1·947 (8) [2]
⟨Ta(1)—X⟩	1·915	⟨Ta(4)—X⟩	1·944
Ta(2)—X(5)	1·868 (11)	Ta(5)—X(1)	2·067 (12)
—X(6)	1·961 (13)	—X(2)	2·005 (12)
—X(9)	1·957 (13)	—X(3)	1·845 (10)
—X(10)	2·036 (13)	—X(5ⁱⁱ)	1·941 (11)
—X(15)	1·960 (7) [2]	—X(13)	2·000 (7) [2]
⟨Ta(2)—X⟩	1·957	⟨Ta(5)—X⟩	1·976
Ta(3)—X(3ⁱ)	1·940 (10)	Ta(6)—X(18)	2·130 (9) [2]
—X(4ⁱ)	1·989 (11)	Ta(6)—X(18ⁱⁱⁱ)	2·891 (8) [2]
—X(9)	1·938 (12)	⟨Ta—Ta⟩	3·753
—X(11)	2·002 (12)	⟨Ta—K⟩	3·825
—X(14ⁱ)	1·965 (8) [2]	K(1)—K(2)	3·894 (4)
⟨Ta(3)—X⟩	1·967		
K(1)—X(2)	3·306 (12)† [2]	K(3)—X(1)	2·725 (13) [2]
—X(3)	2·879 (12)† [2]	—X(1ⁱ)	3·472 (12)† [2]
—X(4)	3·031 (12) [2]	—X((2)	3·367 (12)† [2]
—X(7)	2·756 (12) [2]	—X(5)	3·051 (11) [2]
—X(13)	3·657 (7)†	—X(6)	2·954 (13) [2]
—X(14)	2·979 (8)	—X(13)	3·042 (7)
—X(16)	3·366 (7)†	—X(13ⁱ)	3·285 (7)†
—X(18)	2·679 (9)	—X(15)	2·843 (7)
⟨K(1)—X⟩	2·874	—X(16)	3·410 (7)†
		⟨K(3)—X⟩	2·918
K(2)—X(4ⁱⁱ)	2·866 (11) [2]	K(4)—X(9)	3·264 (12)† [2]
—X(7)	2·874 (13) [2]	—X(10)	2·897 (12) [2]
—X(8)	3·115 (10) [2]	—X(11)	3·744 (12)† [2]
—X(11ⁱ)	3·561 (12)† [2]	—X(12)	2·758 (12) [2]
—X(14ⁱⁱ)	3·314 (8)†	—X(12ⁱ)	3·091 (12) [2]
—X(16)	3·273 (7)†	—X(15)	3·757 (7)†
—X(17)	3·564 (8)†	—X(17)	3·466 (8)†
—X(18)	3·346 (9)†	—X(17ⁱⁱ)	3·471 (8)†
—X(18ⁱⁱ)	3·345 (9)†	⟨K(4)—X⟩	2·915
⟨K(2)—X⟩	2·952		
X(1)—X(2)	2·722 (17)	X(6)—X(15)	2·605 (15) [2]
X(1)—X(5ⁱⁱ)	2·803 (16)	X(6)—X(16)	2·623 (16) [2]
X(1)—X(13)	2·505 (14) [2]	X(7)—X(8)	2·692 (14)
X(2)—X(3)	2·831 (16)	X(7)—X(16)	2·849 (15) [2]
X(2)—X(6)	2·604 (18)	X(8)—X(10)	2·868 (15)
X(2)—X(7)	2·720 (17)	X(8)—X(11ⁱ)	2·720 (15)
X(2)—X(13)	2·851 (14) [2]	X(8)—X(16)	2·664 (12) [2]
X(2)—X(16)	2·737 (14) [2]	X(8)—X(17)	2·721 (12) [2]
X(3)—X(4)	2·664 (15)	X(9)—X(10)	2·647 (16) [2]
X(3)—X(5ⁱⁱ)	2·747 (15)	X(9)—X(11)	2·878 (16)
X(3)—X(9ⁱⁱ)	2·808 (16)	X(9)—X(14ⁱ)	2·973 (14) [2]
X(3)—X(13)	3·034 (13) [2]	X(9)—X(15)	2·934 (14) [2]
X(3)—X(14)	2·710 (13) [2]	X(10)—X(12ⁱ)	2·647 (17)
X(4)—X(11ⁱⁱ)	2·770 (16)	X(10)—X(15)	2·952 (14) [2]
X(4)—X(14)	2·560 (13) [2]	X(10)—X(17)	2·905 (14) [2]
X(5)—X(6)	2·800 (17)	X(11)—X(12)	2·749 (17)
X(5)—X(9)	2·701 (16)	X(11)—X(14ⁱ)	2·830 (14) [2]
X(5)—X(13ⁱ)	2·723 (13) [2]	X(11)—X(17ⁱⁱ)	2·595 (15) [2]
X(5)—X(15)	2·601 (13) [2]	X(12)—X(17ⁱⁱ)	2·783 (15) [2]
X(6)—X(8)	2·728 (16)	X(18)—X(18ⁱ)	2·707 (17)
X(6)—X(10)	2·903 (17)	X(18)—X(18ⁱⁱ)	2·707 (17)
		⟨X—X⟩	2·722

Symmetry code: (i) ȳ, x − y, z; (ii) y − x, x̄, z; (iii) x, y, z + 1.

* The numbers in square brackets indicate the number of equal distances.

† These distances are not included in the mean.

trigonal prism having average distances of 2·952 and 2·915 Å respectively (Fig. 3). Only distances <3·20 Å were considered in these averages. Similar coordinations and average distances were found in $K_2Ta_4F_4O_9$ ($⟨K—X⟩ = 2·960$ Å) and $K_6Ta_{6·5}F_{9·5}O_{14·5}$ ($⟨K—X⟩ = 2·881$ and 2·969 Å).

The sublattice $[Ta_{0·5}X_3]_n$

The infinite chain $[Ta_{0·5}X_3]_n$ is made up of anionic (O, F) trigonal prisms sharing faces along [001] (Fig. 4). The height of each prism is equal to c (3·878 Å). In this chain the Ta atoms [Ta(6)] are statistically distributed on the twofold site 2(*i*) with a 25% occupancy, *i.e.* a half-atom per unit cell. This statistical occupancy is necessitated by the very short c axis, where the maximum occupancy can only be 50% (of course only one of the positions of the twofold site can be occupied at one time). The displacement of Ta(6) from the ideal center of the prism should be noted; this is necessary for the formation of stronger bonds with three of its anionic neighbors [X(18)].

In the trigonal prism the Ta—X distances are 2·130 and 2·891 Å (Fig. 5). Significant bond formation seems, therefore, to take place only with three of the six neighboring anions. This phenomenon was also observed in $K_6Ta_{6·5}F_{9·5}O_{14·5}$ where identical trigonal-prismatic chains were found.

The interpenetration of the two sublattices together with the K^+ ions gives rise to the three-dimensional structure with the general formula $K_{12}Ta_{15·5}X_{54}$.

Fig. 3. Coordination polyhedra of the potassium ions (distances are given in Å).

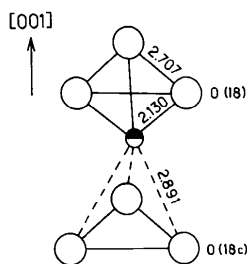Fig. 4. Trigonal-prismatic chains along the [001] direction.

Fig. 5. The anionic environment of Ta(6) (distances are given in Å).

$K_6Ta_{6.5}F_{9.5}O_{14.5}$ and $K_{12}Ta_{15.5}F_{18.5}O_{35.5}$ have practically identical infinite tunnels in their frameworks (tunnel B) filled with six K^+ ions and a similar sublattice $[Ta_{0.5}X_3]_n$. This sublattice, to within experimental error, is identical in both cases, except that in the present work no rotational disorder around z was observed for the trigonal prism. This may be explained by the formation of strong bonds with three of the six K^+ ions in the tunnel $[K(1)-X(18) = 2.679 \text{ Å}]$.

A study is in progress to determine the homogeneity range in both the $K_6Ta_{6.5}F_{9.5}O_{14.5}$ and $K_{12}Ta_{15.5}F_{18.5}O_{35.5}$ phases due to the partial occupation of the $2(i)$ site by Ta atoms.

References

AWADALLA, A. A. & GATEHOUSE, B. M. (1978). *J. Solid State Chem.* **24**, 349–355.

BOUKHARI, A., CHAMINADE, J. P., VLASSE, M. & POUCHARD, M. (1979). *Acta Cryst.* B35, 1983–1986.

BUSING, W. R., MARTIN, K. O. & LEVY, H. A. (1962). *ORFLS.* Report ORNL-TM-305. Oak Ridge National Laboratory, Tennessee.

CHAMINADE, J. P., VLASSE, M., POUCHARD, M. & HAGENMULLER, P. (1974). *Bull. Soc. Chim. Fr.* (9–10), 1791–1794.

DAUBEN, C. H. & TEMPLETON, D. H. (1962). *International Tables for X-ray Crystallography*, Vol. III, p. 214. Birmingham: Kynoch Press.

McMASTER, W. H., KERR DEL GRANDE, N., MALLET, J. H. & HUBBEL, J. H. (1969). *Compilation of X-ray Cross Sections*, UCRL-50174, Sect. II, Rev. I. Washington: National Bureau of Standards.

PERRON-SIMON, A., VON DER MÜHLL, R., RAVEZ, J. & HAGENMULLER, P. (1977). *Mater. Res. Bull.* **12**, 543–547.

POUCHARD, M. & HAGENMULLER, P. (1978). *Solid Electrolytes*, edited by P. HAGENMULLER & W. VAN GOOL. New York: Academic Press.

VLASSE, M., BOUKHARI, A., CHAMINADE, J. P. & POUCHARD, M. (1979). *Mater. Res. Bull.* **14**, 101–108.

VLASSE, M., CHAMINADE, J. P., MASSIES, J. C. & POUCHARD, M. (1975). *J. Solid State Chem.* **12**, 102–109.

VLASSE, M., CHAMINADE, J. P. & POUCHARD, M. (1973). *Mater. Res. Bull.* **8**, 117–126.

VLASSE, M., CHAMINADE, J. P. & POUCHARD, M. (1976). *Bull. Soc. Fr. Minéral. Cristallogr.* **99**, 3–7.

VLASSE, M., CHAMINADE, J. P., SAUX, M. & POUCHARD, M. (1977). *Rev. Chim. Minér.* **14**, 429–434.

(4H)₃-6C-Type Superstructure of TiS₁.₅₁ as Revealed by High-Resolution Electron Microscopy

By Y. BANDO, M. SAEKI, M. ONODA AND I. KAWADA

National Institute for Researches in Inorganic Materials, Sakura-mura, Niihari-gun, Ibaraki 300-31, Japan

AND M. NAKAHIRA

Okayama College of Science, Laboratory of Solid State Chemistry, Ridai-cho, Okayama 700, Japan

Abstract

The $(4H)_3$-6C-type superstructure of $TiS_{1.51}$ is examined by 100 kV high-resolution electron microscopy. The crystal has monoclinic symmetry (pseudohexagonal) with lattice parameters $a = 10.3$, $b = 5.92$, $c = 34.9$ Å and $\beta = 90°$. The space group is Cc. The metal vacancies are confined to every second metal layer and ordered within the layers, resulting in the formation of a superstructure. They are arranged in a stacking sequence of the $6C$ type along the c axis, while S atoms have a $4H$-type arrangement. It is shown that faults in the stacking of the metal-vacancy layers are present.

The titanium–sulfur system has a variety of structures in the range between TiS and TiS_2 (Jeannin, 1962).